A Novel ANN-Based GMPPT Method for PV Systems Under Complex Partial Shading Conditions

Ye, Song-Pei; Liu, Yi-Hua; Pai, Hung- Yu; Sangwongwanich, Ariya; Blaabjerg, Frede

Published in:
IEEE Transactions on Sustainable Energy

DOI (link to publication from Publisher):
10.1109/TSTE.2023.3284866

Publication date:
2024

Document Version
Accepted author manuscript, peer reviewed version

A novel ANN-based GMPPT method for complex partial shading conditions

Song-Pei Ye, Yi-Hua Liu *Member, IEEE*, Hung-Yu Pai,
Ariya Sangwongwanich *Member, IEEE* and Frede Blaabjerg, *Fellow, IEEE*

***Abstract*—In this paper, a new two-stage global maximum power point tracking (GMPPT) algorithm based on artificial neural network (ANN) is proposed. A novel ANN architecture is presented first, which requires fewer sampling points than other ANN-based GMPPT approaches, thereby reducing both the tracking time and power loss. The proposed GMPPT method features high tracking speed and accuracy and does not require expensive irradiance sensors or temperature sensors. Also, it can be realized using a low-cost digital signal controller due to its low computational complexity. To verify the effectiveness of the proposed method, the simulations of 252 shading patterns (SPs) which take operating temperature into account, as well as the simulations and experiments of 3 complicated SPs are carried out respectively. According to the simulation results, the proposed method has the best performance among all methods in terms of tracking speed, tracking accuracy, and tracking loss for all the three tested SPs. The simulated results of 252 SPs show that the performance indexes (PIs) of the proposed method are the best among all the compared methods, which are: the average tracking time 0.18 seconds, average power loss 0.01 W. In addition, the proposed method can correctly predict the GMPP positions of all 252 SPs. Furthermore, the PIs of the proposed method are also the best among all the compared methods according to the experimental results, which are: the tracking speed 0.21 seconds, tracking accuracy 99.66%, and tracking loss 12.58 W, all the above are average values.**

***Index Terms*—Artificial Neural Network (ANN), Global Maximum power point tracking (GMPPT), Photovoltaic (PV)**

I. Introduction

In recent decades, renewable energy systems, particularly PV, have attracted more interest owing to their abundant and environmentally-friendly characteristics. Because of the nonlinear relation between the P–V characteristics, a circuit is necessary to make the PV array operate at the voltage corresponding to the maximum power. This can be realized by using a DC-DC converter equipped with a maximum power point tracking (MPPT) technology. Traditional MPPT methods, e.g., hill-climbing (HC), perturbation and observation (P&O), and incremental conductance (INC) are the algorithms that feature easy realization and wide application. However, a photovoltaic generation system (PGS) is usually composed of many solar panels in series and parallel. The irradiance and temperature of each solar panel will vary due to the solar angle or the position of the shade, resulting in a partial shading condition (PSC). When the system is in PSC, the output power-voltage characteristic curve of the system will change from a simple single-peak graph to a complex multi-peak one with multiple local maximums. Under this circumstance, the conventional MPPT method may operate on local maximum power point (LMPP) instead of the global MPP (GMPP). This situation will lead to an obvious loss in output power, resulting in lower utilization of the system. Hence, it is importance to use the GMPPT method to find the GMPP [1]-[5].

To deal with PSC, specially designed GMPPT algorithms are typically required [6]-[32]. These methods can be categorized as follows: (1) direct search methods; (2) two-stage methods, and (3) soft computing-based methods. In direct search methods, [6] utilizes the generalized pattern search method. By repeatedly expanding or narrowing the location interval of the voltage operating point (OP), GMPPT can be thereby realized. In [7], the Fibonacci search method is employed to calculate the GMPP iteratively. In [8], a new solar cell model-based method is proposed to extract the GMPP. In [9], a modified maximum power trapezium (MPT) method for GMPPT is proposed. In comparison with the conventional MPT method, the proposed method provides a variable current range lower bound by utilizing the monotonic output characteristics of the PV panel. In [10], the DIRECT (Dividing Rectangles) method is adopted to obtain the GMPP by dividing the searching domain systematically into hyperrectangles with smaller sizes. In [11], a novel GMPPT algorithm is proposed based on the rectangular power comparison (RPC), which utilizes the basic relationships among the shading factor and bypass diode voltage to obtain the GMPP. [12] presents a deterministic particle swarm optimization (DPSO) technique to improve the tracking efficiency of the conventional particle swarm optimization (PSO) algorithm. The objective is to remove the random numbers, which serve as the accelerations factor in the PSO's velocity equation. Even though this method is based on PSO, it can be seen as a new type of direct method because the random numbers are removed.

Regarding the two-stage methods, a first stage is utilized to find all the possible "candidate intervals" of GMPP. Then, a second stage is used to search for the exact location of the GMPP. Among this category, [13] adopted a fixed-spacing segmentation, [14] utilized restrictive voltage windows, and [15] applied a search-and-skip process to find the candidate interval. In the second stage, the P&O method [13], [14], and quadratic equation [15] are employed. In terms of such methods, the choice of the first-stage method will affect the accuracy of "candidate intervals" where GMPP is obtained under different SPs. The second stage of the method will

influence the tracking speed and steady-state tracking accuracy. For SC-based methods, PSO [16], [17], cuckoo search (CS) [18], firefly algorithm [19], artificial bee colony (ABC) [20], and grey wolf optimization (GWO) [21] are applied to find the real GMPP. Since the SC method can properly deal with complex optimization problems with multiple peaks, the SC-based method accounts for the largest proportion of the recent GMPPT algorithms. However, since these SC-based methods are all stochastic, the acquired GMPP and the iteration number needed for obtaining the final solution vary for each trial run. Moreover, due to the high iteration number required for obtaining MPP, the tracking speed of these techniques is slow under uniform insolation conditions (UIC) and PSC.

As it can be seen from the above description, the two-stage method features fast tracking speed, but the method selected in the first stage will affect its performance. This paper proposes a novel two-stage GMPPT method. The first stage uses an ANN to obtain the location of GMPP under different PSCs. Compared with other SC methods, which require random numbers and iterative operations for searching GMPP, ANN only needs simple multiplication and addition for GMPP calculation; hence, it is suitable to be implemented by low-cost DSC. In addition, the ANN-based method does not need to use random numbers, which makes the tracking time fixed and the tracking speed fast. The second stage of the GMPPT method proposed in this paper adopts the alpha-P&O method [22], which can effectively solve the trade-off problem regarding tracking speed/tracking accuracy. Nowadays, many works of literature are adopting ANN to estimate the GMPP location [23-30]. In terms of the ANN architecture used in the first stage, [23] measures the voltage and current values of specific positions as the input data of the ANN and uses the voltage of GMPP (denoted as V_{GMPP}) as the output. [24] uses the irradiances of each solar panel under a specific SP as the input data of the ANN, and the V_{GMPP} is used as the output. In [25], the authors take 0.8 times the open-circuit voltage of a single solar panel ($V_{OC,\,cell}$) as the measurement interval and uses the measured voltage and current values as the input of ANN; also, the V_{GMPP} is used as the output. [26] measures the power value of distinct points and calculates the power slope (dP) value of these points; then, the obtained value is used as the input of ANN, and the V_{GMPP} is the output. [27] measures the short-circuit current and open-circuit voltage based on the number of solar panels connected in series under different irradiance levels (ILs) as the input of ANN, and the output is also V_{GMPP}. In [28], the author uses the irradiances of each solar panel under a specific SP as the input data of the ANN, and the output is the maximum (V_{max}) and minimum (V_{min}) voltage values of the interval where the GMPP is located, and one of them is chosen as the starting point of the next stage. The input and output of [29] are the same as those of [28], the difference is that the starting point of the second stage selects the average value of the two voltage values (V_{avg}) outputted by the ANN, thereby speeding up the tracking speed. Finally, [30] divides the solar panel into groups and calculates the average ILs of each group as the input of ANN after measuring the irradiance of each solar panel under a specific SP. At last, it directly outputs the V_{GMPP} and the power value of the GMPP. In terms of the methods used in the second stage, [26], [28] uses the P&O method, [23], [25] utilizes the INC method, [27] utilizes the HC method, and [24], [29], [30] employs the variable step method. Generally, using a variable step method in the second stage improves tracking accuracy.

In this study, the proposed technique has been simulated and realized in MATLAB/Simulink and a real system respectively to present a fair comparison between the GMPPT techniques. The simulation of different GMPPT techniques is performed under 252 different SPs, which take operating temperature into account. Simulation results showed that the tracking performance of the proposed two-stage ANN-based method outperformed other GMPPT techniques. The main contributions of this study are listed as follows:

- It proposes a new two-stage GMPPT algorithm based on ANN, featuring simple implementation, fast convergence, high accuracy, etc.
- It requires fewer sampling points than other ANN-based GMPPT approaches, thereby enhancing both the tracking speed and power loss.
- It prevents oscillations around the GMPP and reduces the power loss in the PGS.
- It has low computational complexity; hence, it can be realized by a low-cost DSC. Furthermore, the proposed method does not require expensive irradiance sensors and temperature sensors
- The simulation results of 252 SPs, which take operating temperature into account, are provided. These results can be used to effectively evaluate the pros and cons of each method.
- Compared with the other ANN architectures for GMPP estimation presented in the literature, the proposed ANN has the highest estimation accuracy, it can correctly predict the GMPP positions of all 252 SPs.
- The absolute error value between the OP predicted by the proposed ANN and the real V_{GMPP} can be reduced to 0.04 V on average, which can greatly reduce the tracking time required for the 2nd-stage α-P&O method to reach the real GMPP.

II. PV Model and Partial Shading Problem

A. Basic Characteristics of a PV Cell

In this study, an equivalent one-diode circuit model illustrated in Fig. 1 is utilized to stand for the electrical behavior of a PV cell. In addition to a current source I_g and a diode D within the equivalent model, a shunt resistance R_p is also taken into account to represent the leakage current and a series resistance R_s describing the resistance inside an individual cell as well as the resistance between two cells. Based on Fig. 1, the current I_p can be acquired by subtracting the diode current I_D from the photocurrent I_g:

$$I_p = I_g(S,T) - I_s(T)\left(e^{\frac{q(R_s I_p + V_p)}{KATN}} - 1\right) - \frac{R_s I_p + V_p}{R_p} \quad (1)$$

In (1), I_s represents the saturation current; q is the electron charge; R_s stands for the equivalent series resistance; R_p represents the equivalent shunt resistance; N is the diode ideality factor; K is the Boltzmann's constant, and A stands for the diode ideality factor. T is the cell temperature in Kelvin, which can be calculated as follow:

$$T_{cell} = T_{air} + \frac{NOCT - 20}{80} \cdot S \quad (2)$$

In (2), T_{air} stands for the ambient air temperature, $NOCT$ is the Nominal Operating Cell Temperature, and S represents the current IL.

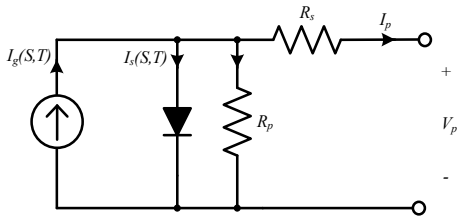

Fig. 1. Equivalent circuit of the PV cell utilized in this study.

B. Effect of PSC on PGS

PGS is composed of several PV modules connecting in parallel or in series, where a single PV module consists of several PV cells. Depending on the required specification, a higher terminal voltage/output current of the PV module can be acquired from the series/parallel connection of PV cells. Under PSC, multiple peaks on the P–V curve may occur owing to the conduction of bypass diodes, and this phenomenon becomes apparent in series-connected PV modules. According to the literature, the P–V characteristic curves of distinct shading patterns (SPs) are different from one to another and the GMPP can be located in either the low-voltage or high-voltage ranges. Therefore, most conventional MPPT algorithms cannot track GMPP successfully when PSC is encountered.

III. Description of The Proposed Method

The skill proposed by this study firstly uses an ANN to estimate the voltage of the GMPP under current IL, then utilized the α-P&O MPPT method to track the real MPP. This section will first introduce the ANN-based GMPP estimation method and then describe the way to conduct α-P&O MPPT.

A. Neural Network Design and Implementation

Fig. 2 shows the architecture of the proposed ANN, and it is explained as follows. This study designed a four-layered neural network architecture, including one input layer, two hidden layers, and one output layer, respectively. The neural network input parameters used by this study are the current values I_1, I_2, I_3, I_4, and I_5 of the five flat intervals in the I-V curve as shown in Fig. 3. The flat interval is defined as the interval where the difference between the highest and lowest current values measured under a specific irradiance is within 1%. To ensure that the measured current values are all within the defined flat intervals, the sampling current at $(0.3+(i-1)V_{OC})$ is selected as the input in this study, where V_{OC} is the open circuit voltage of a single solar panel, i=1~N, N is the number of solar panels in series; the output of ANN is the LMPP voltages (V_{LMPP}) and their corresponding power in each region under the specific SP; the two Hidden Layers contain 10 neurons respectively, and the activation function is Tansig, as shown in (3). Levenberg–Marquardt method is used as the training method in this study.

$$y(n) = \frac{e^n - e^{-n}}{e^n + e^{-n}} = \text{Tansig}(n) \quad (3)$$

The accuracy of the ANN is directly related to the completeness of the training set. In the following, the method of generating the training set of the proposed ANN will be described in detail. Fig. 4 is the flow chart showing the generation of the ANN training data in this study. First, use the five flat intervals current values I_1~I_5 for each of the 252 different irradiance combinations as the input of the ANN. Then, MATLAB is used to conduct the simulation of the α-P&O method to find out the V_{LMPP} of each region and its corresponding power; these values will be recorded and used as the output of the ANN training data.

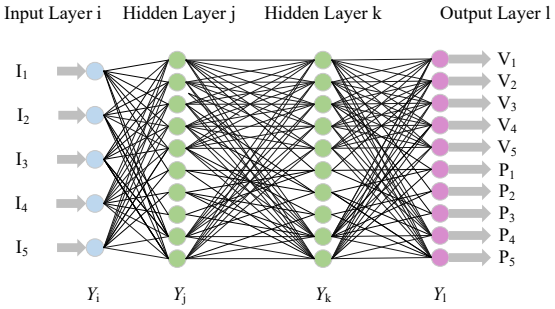

Fig. 2. ANN architecture proposed in this study.

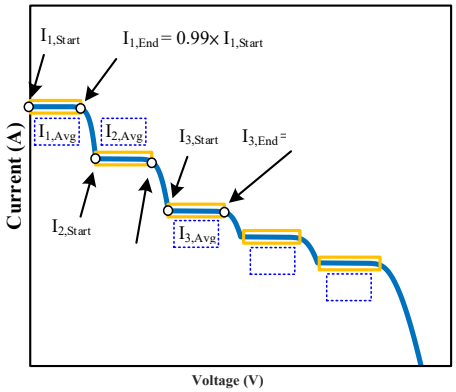

Fig. 3. Illustration of the current sampling position of the proposed method.

B. The Utilized α-P&O Method

The first-stage method proposed in this paper has been able to track the vicinity of the GMPP point; however, considering that there are still errors in part of the SPs and to improve the steady-state tracking accuracy, this study used the α-P&O method proposed in [22] in the second stage to locate the precise location of the GMPP during the second stage. The α-P&O method utilizes the maximum possible voltage perturbation step (VPS, V_{step}) at the beginning. When the OP

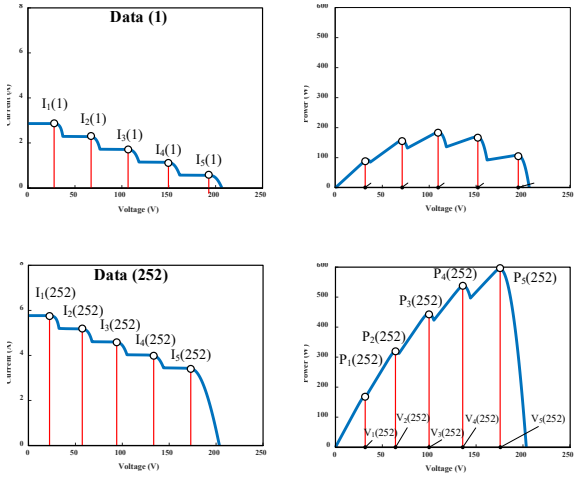

Fig. 4. Training data set acquisition method of the proposed technique.

passes the MPP, the tracking direction is reversed, and the VPS is multiplied by a constant α (α < 1) to reduce the step size, as depicted in (4).

$$V_{step,new} = \alpha \cdot V_{step,old} \tag{4}$$

Based on the operating principle of the P&O method, this algorithm perturbs the MPP repeatedly. As a result, the VPS in (4) will gradually decrease until the minimum VPS (V_{crit}) allowed by the system is reached. In this study, the value of α and the initial V_{step} are set as 0.5 and 1 V, respectively.

C. Flow Chart of Proposed Method

The proposed two-stage GMPPT method boasts advantages such as high tracking speed, high tracking accuracy, low tracking loss, etc. Fig. 5 depicts the flow chart of the proposed method. As Fig. 5 illustrates, the proposed method will first detect the five current values and input the obtained five current values to the trained ANN to acquire the corresponding operating voltages of the five LMPPs (including GMPP) and their corresponding powers. Then, the program will find the largest one from the five candidate powers and set its corresponding voltage value as the initial OP of the second stage. Lastly, the α-P&O MPPT algorithm is executed to converge the OP to GMPP.

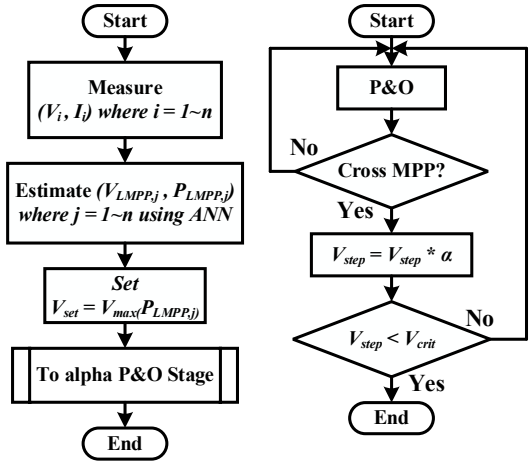

Fig. 5. Flow chart of the proposed method.

IV. Simulation and Experimental Results

A. Description of the Test Conditions

A key to having a good performance in a two-stage GMPPT technique is closely related to whether the correct candidate intervals can be found in the first stage. Therefore, this study first compares the performance of the ANN architectures used in the first stage which are proposed in the literature. Generally, there are three aspects to evaluate the performance of ANN: the first is the amount of input data required by ANN. The excessively large amount of input data indicates that plenty of time and computing resources are required to collect training data during the initial ANN training phase. Meanwhile, the amount of input data also represents the number of OPs that need to be sampled during the experiment. If the number of the first-stage sampling points is large, the tracking time will also become longer, which will lead to an increase in tracking loss. The second is the accuracy rate of ANN (***ANN$_{AR}$***). Its definition is the number of correct predictions divided by the total number of predictions, as depicted in (5). A higher ***ANN$_{AR}$*** indicates that the selected input/output data and/or the ANN architecture are relatively better choices. Finally, the ***MSE*** (mean-square error) value is calculated for the error between the results obtained by ANN and the real ones for a certain number of problems, as shown in (6). An large ***MSE*** value means that the results obtained by the ANN are far from the correct answer, indicating that the selected input/output data and/or the ANN architecture is not suitable for handling this kind of problem.

$$ANN_{AR} = \frac{Prediction_{correct}}{Prediction_{total}} \tag{5}$$

$$MSE = \sqrt{\frac{\sum_{i=1}^{N}(P_{predict,i} - P_{real,i})^2}{N}} \tag{6}$$

Since the PGS tested in this study is a 5S1P system, according to the literature, the P−V curve will show five peaks when the ILs of the five solar panels in the system are all different [31]. This is the most complicated P−V characteristic curve in the 5S1P system. In this study, non-repeatable irradiance tests are adopted to validate the GMPPT performance. It is to make all series-connected solar panels in the system under different ILs. In this study, the possible ILs are 100 W/m^2~ 1000 W/m^2, with an interval of 100 W/m^2. Namely, each solar panel is likely to be exposed to ten possible ILs. As a result, the possible number of SP combinations of the 5S1P system is C(10, 5) = 252. In addition, since the operating temperature is different when the solar panel receives different IL, it can be expressed by the *NOCT* shown in (2).

Table I summarizes the training results of the compared 8 ANN approaches and the proposed ANN method. For the sake of fairness, the training data used by all methods are all the same 252 SPs that consider the operating temperature. Hence, there are 252 training data (252 input and output vectors). Take [23] as an example, the input is the voltage and current sampling under 252 SPs at [0.8 V_{OC}, 1.6 V_{OC}, 2.4V_{OC}, 3.2V_{OC}, and 4.0 V_{OC}] as described in [23], and the output is the V_{GMPP} of each SP. The input and output data of other methods can also be

obtained according to the description of each method in the original paper, and will not be elaborated on here. Take [23] as an example; since its input is the voltage and current pairs at [0.8 V_{OC}, 1.6 V_{OC}, 2.4V_{OC}, 3.2V_{OC}, and 4.0 V_{OC}], five points need to be sampled. The N_{SP} for other ANN methods can be deduced by analogy. It can be seen from Table I that the performance of the proposed ANN-based method is the best in terms of ANN_{AR}, *MSE*, and N_{SP}. Therefore, compared with the ANN presented in other works of literature, the ANN proposed in this study is more suitable for the first stage of the two-stage GMPPT method. In addition, no irradiance and/or temperature information are required.

To further verify the effectiveness and correctness of the proposed method, this study will first compare the proposed method to the other four state-of-the-art methods proposed in recent literature, as described in the following: the method presented in [32] (direct method, denoted as the DC method), the method described in [20] (soft computing method, denoted as ABC method), the method presented in [16] (soft computing method, denoted as PSO method), and the method described in [26] (two-stage method, denoted as ANN_{old}. The reason for choosing ANN_{old} method is that the method's ANN_{AR} is the best among the eight compared ANN methods. The test of the five methods is initially implemented with three distinctive SPs, and the simulated and measured waveforms will be offered as well. Secondly, to fairly assess the performance of various GMPPT methods under different SPs and compare their pros and cons, this study will adopt the 252 SPs, which consider the operating temperature, with non-repeatable ILs as the test conditions and provide complete statistical simulation results.

TABLE I
THE COMPARISON BETWEEN THE PROPOSED ANN AND THE ONES IN THE LITERATURE FOR GMPP TRACKING

Method	Input	Output	ANN_{AR}	*MSE*	N_{SP}
[23]	V*5, I*5	V_{mpp}	210	195	5
[24]	G*5	V_{mpp}	205	131	5
[25]	V*5, I*5	V_{mpp}	185	231	5
[26]	dP*9, P*9	V_{mpp}	236	221	27
[27]	V_{oc}*1, I*5	V_{mpp}	227	101	6
[28]	G*5	V_{min}, V_{max}	156	164	5
[29]	G*5	V_{min}, V_{max}	234	202	5
[30]	V_{avg}, G*3	V_{mpp}, P_{mpp}	166	390	5
Proposed	I*5	V_{mpp}	252	0.045	5

B. Simulation Result

Fig. 6 shows the block diagram of the proposed GMPPT system; this study utilizes MATLAB/SIMULINK to establish a simulation platform. Table II and Table III list the parameters used in the simulation; Fig. 7 illustrates the tested SPs. In Fig. 7, the ILs of pattern A are [100 W/m^2, 200 W/m^2, 300 W/m^2, 600 W/m^2, and 1000 W/m^2]; the ILs of pattern B are [100 W/m^2, 200 W/m^2, 600 W/m^2, 800 W/m^2, and 900 W/m^2]; the ILs of pattern C are [300 W/m^2, 500 W/m^2, 700 W/m^2, 900 W/m^2, and 1000 W/m^2]. In Fig. 7, it can be observed that the GMPP of pattern A locates in the 2nd peak; the GMPP of pattern B locates in the 3rd peak; the GMPP of pattern C locates in the 4th peak, and the 3rd peak has a smaller but similar value to GMPP. Fig. 8-10 present the tracking waveforms of the five compared methods under the three tested SPs. In Fig. 8-10, the total simulation time is 1 second, and the MPPT is implemented every 0.01 seconds for all five methods. The key performance data of the waveforms are summarized in Table IV. In Table IV, Tracking time (***TT***) indicates the required time to track a steady-state (power variation <1%). Tracking accuracy (***TA***) indicates the ratio of the obtained steady-state power to the real GMPP of the current SP. Tracking power loss (***TPL***) indicates the integral of the power difference between the OP and the GMPP of the current SP during the tracking process then divided by the total tracking time. It is worth noting that the results obtained by the SC-based methods may not be the same for each simulation due to their stochastic nature. Hence, the simulation of the ABC and the PSO method in Table IV is executed 100 times, and the obtained results are expressed in the form of mean and standard deviation values (***SDV***). Based on Fig. 8-10 and Table IV, it can be discovered that the ***TA*** of the ABC and the PSO method under Pattern A are both lower than 98.6 %, while their ***TT*** and ***TPL*** are all greater than 0.45 s and 49 W for all the three tested patterns. Although the DC method (modified from the cuckoo search method) removes the randomness in the original method to improve its tracking speed; however, the problem of the direct tracking method is that when faced with a more complicated pattern, it is easy to fall into the local maximum. As shown in Fig. 10, the GMPP of pattern C is in the 4th peak, and the result tracked by the DC method is in the 3rd peak. Although the difference between the tracked power value and the real GMPP value is not large; however, due to the long time-

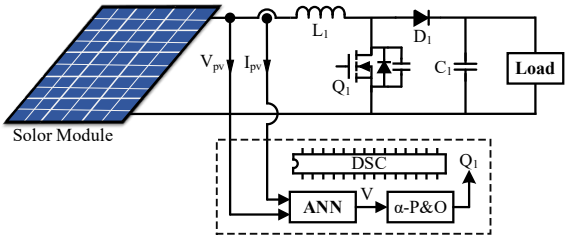

Fig. 6. The block diagram of the proposed GMPPT system.

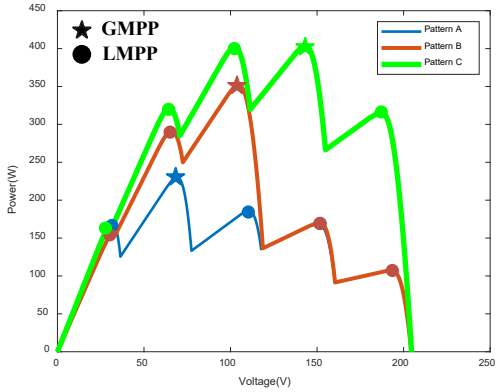

Fig. 7. The three tested shading patterns.

TABLE II
SPECIFICATION OF THE UTILIZED BOOST CONVERTER

Parameters	Boost Converter
Switching frequency	100 kHz
Sampling time	100 kHz
Input inductor	746 μH

Power Switches	IPP200N25N3
Filter capacitor	1000 μF

TABLE III
SPECIFICATION OF THE UTILIZED SOLAR PANEL

Parameters	Value
Maximum PV Power	1000 W
Voltage at MPP	185.55 V
Current at MPP	5.39A
Open circuit voltage, V_{oc}	228.4 V
Short circuit current, I_{sc}	5.69 A

constant of the SP changes, the time being in a steady state is longer than the transient time (the time a SP changes to another SP). Therefore, the accumulated power loss will be considerable in the long run if the real GMPP location cannot be tracked. Finally, in terms of the ANN_{old} method, it is known from Table I that this method requires more samples to operate. Consequently, although the method can track the correct GMPP for both patterns A and B, more required samples lead to a longer tracking time, thereby increasing the power loss of the overall tracking process. Additionally, the importance of $\boldsymbol{ANN_{AR}}$ and ***MSE*** can be seen from the tracking process of pattern C. In terms of pattern C, the ANN_{old} method tracks the wrong interval (3 instead of 4) in the first stage, and the output OP is far from the LMPP of interval 3, resulting in longer time to reach a steady state in the second stage. Moreover, the power loss will accumulate over time, resulting in an overall ***TPL*** greater than 68W, which is even worse than the ABC method. From Table IV, it can be observed that in patterns A, B, and C, the ***TT***, ***TA***, and ***TPL*** of the method proposed in this study are all in the first place. The average ***TT***, ***TA***, and ***TPL*** of the three patterns are 0.19 s, 99.99 %, and 11.10 W respectively. In comparison with the DC, ABC, PSO, and ANN_{old} methods, the proposed method can reduce the ***TT*** by 9.52 %, 65.45 %, 62.75 %, and 68.85 %, respectively; increase the ***TA*** by 0.15 %, 2.05 %, 0.62 %, and 6.46 %, respectively; improve the ***TPL*** by 12.32 %, 82.45 %, 96.14 %, and 73.71 %, respectively. All the above values are average values.

To further show the superiority of the proposed method, this study compares the performances of the same five methods using the 252 SPs that consider temperature. The comparison results are listed in Table V. In Table V, $\boldsymbol{TT_{avg}}$ indicates the sum of the ***TT*** results for all SPs divided by the total number of tested SPs. Since the real GMPP under different SPs is not identical and the fact that the PGS can obtain high profit once the total power generation is high. Hence, this study defines a PI called average power error (***APE***) to stand for the average tracking accuracy. ***APE*** can be acquired by dividing the sum of the differences between the steady-state power acquired under each SP and the real GMPP by the total number of tested SPs, as presented in (7).

$$APE = \frac{1}{N}\sum_{i=1}^{N}\left[(1-TA_i)\cdot GMPP_i\right] \tag{7}$$

In this equation, $\boldsymbol{TA_i}$ represents the **TA** value of the *i*-th SP; $\boldsymbol{GMPP_i}$ stands for the real GMPP value of the *i*-th SP. Lastly, the correct total (***CT***) in Table 5 stands for the total number of times the steady-state OP voltage obtained under each SP and the real GMPP are on the same peak (i.e., the number of times the tested method correctly finds the GMPP candidate interval for all the SPs).

Based on Table V, it can be observed that the proposed method is quite robust compared with the other four methods. Its $\boldsymbol{TT_{avg}}$, ***APE***, and ***CT*** value all rank first in the 252 SPs which considers the operating temperature. The $\boldsymbol{TT_{avg}}$ indicates that the proposed method simply needs fewer time to track to GMPP. The CT is 252, implying that the proposed method has the highest probability of finding the real GMPP under each possible SP. Likewise, its ***APE*** also ranks first in these test scenarios. Compared with the DC, ABC, PSO, and ANN_{old} methods, the proposed method can improve 99.36%, 99.81%, 99.40%, and 99.65% on average under 252 SPs which take the operating temperature into account.

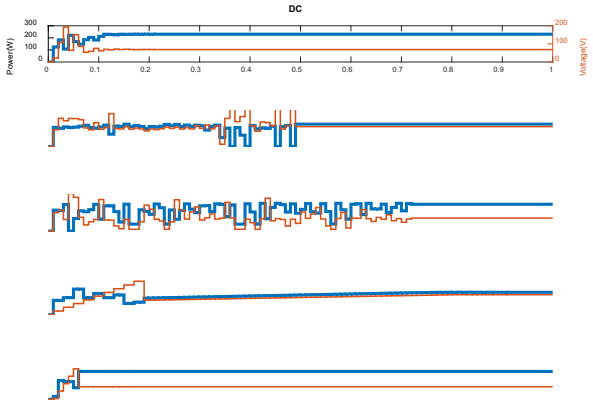

Fig. 8. Tracking waveforms of the five compared methods (Pattern A).

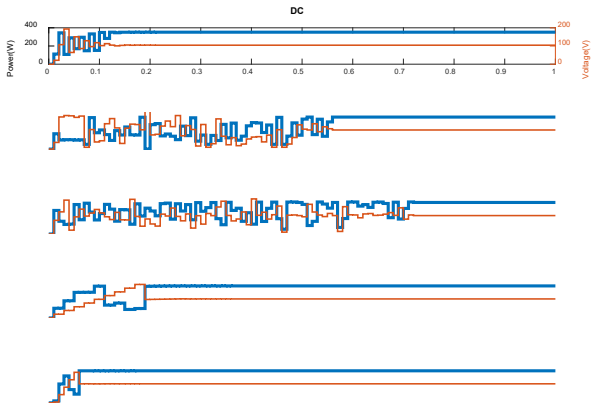

Fig. 9. Tracking waveforms of the five compared methods (Pattern B).

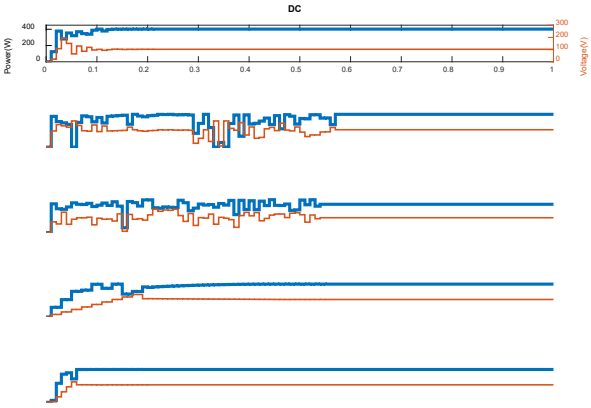

Fig. 10. Tracking waveforms of the five compared methods (Pattern C).

TABLE IV
THE SIMULATION RESULTS OF THE FIVE COMPARED METHODS

Pattern	PI	DC	ABC	PSO	ANN_{old}	Proposed
A	***TT (s)***	0.21	0.56	0.56	0.91	0.18
	SDV	N.A.	0.18	0.13	N.A.	N.A.
	TA (%)	99.98	94.94	98.56	80.62	99.99
	SDV	N.A.	0.08	0.04	N.A.	N.A.
	TPL (W)	8.18	49.63	78.10	68.64	8.14
	SDV	N.A.	19.03	32.57	N.A.	N.A.
B	***TT (s)***	0.21	0.56	0.50	0.36	0.18
	SDV	N.A.	0.18	0.10	N.A.	N.A.
	TA (%)	99.99	99.07	99.81	99.99	99.99
	SDV	N.A.	0.02	0.01	N.A.	N.A.
	TPL (W)	16.49	87.60	122.89	32.85	13.48
	SDV	N.A.	25.41	49.98	N.A.	N.A.
C	***TT (s)***	0.21	0.52	0.46	0.55	0.20
	SDV	N.A.	0.12	0.09	N.A.	N.A.
	TA (%)	99.56	99.81	99.75	99.99	99.99
	SDV	N.A.	0.01	0.01	N.A.	N.A.
	TPL (W)	13.31	52.46	86.56	25.73	11.70
	SDV	N.A.	15.94	46.74	N.A.	N.A.

TABLE V
PERFORMANCE COMPARISON OF FIVE METHODS UNDER 252 SPS

PI	DC	ABC	PSO	ANN_{old}	Proposed
APE (W)	1.56	5.20	1.66	2.82	0.01
SDV	N.A.	0.87	0.44	N.A.	N.A.
CT	231	227.1	239.2	221	252
SDV	N.A.	3.02	4.13	N.A.	N.A.
TT_{avg} ***(s)***	0.19	0.56	0.52	0.51	0.18

C. Experimental Results

To further prove the superiority of the proposed method, this study also conducts experiments on these five GMPPT methods. This study realizes a 400 W prototyping circuit, and the experiments are implemented subsequently. In this paper, a low-cost DSP TMS320F280049 from Texas Instruments is adopted for realizing the GMPPT algorithms. The experiments are carried out with an AMETEK TerraSAS DCS80-15 solar array simulator (SAS) as a power source. The parameter utilized in the experiment is identical to the ones used in the simulation. Fig. 11-13 illustrates the voltage and power tracking waveform in the entire measured time interval (1 second) of the proposed method in the pattern A, B, and C test condition, respectively. Likewise, according to Fig. 11-13, it can be discovered that the experimental results are similar to the ones obtained from the simulation, proving the accuracy of the simulated results. Table VI shows the results of the measured waveforms under these three SPs. It should be noted that the experiments of the ABC and PSO methods in Table VI are only performed 20 times in experiments. In Table VI, it can be observed that the trend of the measured data is consistent with the simulated data listed in Table III. From Table VI, it can be observed that the ***TT***, ***TA***, and ***TPL*** of the method proposed in this study are all in the first place. The average ***TT***, ***TA***, and ***TPL*** of the three patterns are 0.21 s, 99.66 % and 12.58 W, respectively. Compared with the DC, ABC, PSO, and ANN_{old} methods, the proposed method can reduce the ***TT*** by 12.50 %, 65.57 %, 63.16 %, and 67.69 %, respectively; increase the ***TA*** by 1.95 %, 2.39 %, 2.32 %, and 6.42 %, respectively; improve the ***TPL*** by 10.69 %, 82.69 %, 88.50 %, and 75.27 %, respectively. All the above values are average values. Therefore, through the observation of the simulation and experimental results, it can be known that the proposed two-stage ANN-based GMPPT technique is very suitable for handling GMPPT problems.

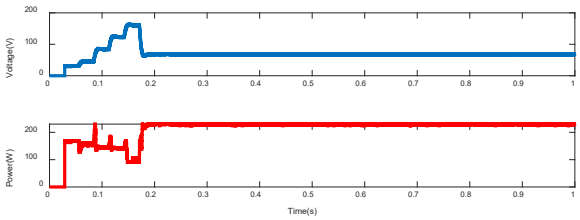

Fig. 11. Tracking waveforms of the proposed method under pattern A

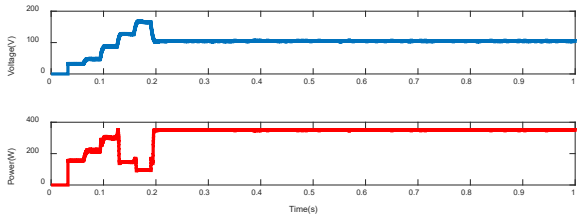

Fig. 12. Tracking waveforms of the proposed method under pattern B

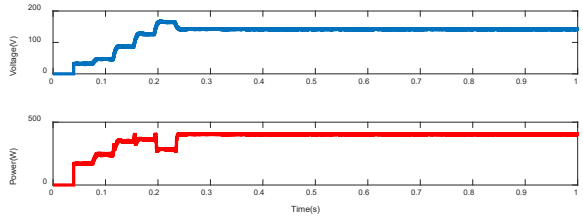

Fig. 13. Tracking waveforms of the proposed method under pattern C

TABLE VI
EXPERIMENTAL RESULTS OF THE FIVE COMPARED METHODS

Pattern	PI	DC	ABC	PSO	ANN_{old}	Proposed
A	***TT (s)***	0.22	0.58	0.57	0.87	0.18
	SDV	N.A.	0.19	0.13	N.A.	N.A.
	TA (%)	95.20	96.43	99.59	84.83	99.69
	SDV	N.A.	0.08	0.04	N.A.	N.A.
	TPL (W)	10.22	63.29	95.76	85.36	10.04
	SDV	N.A.	24.46	39.71	N.A.	N.A.
B	***TT (s)***	0.23	0.63	0.57	0.41	0.20
	SDV	N.A.	0.21	0.11	N.A.	N.A.
	TA (%)	99.19	98.67	95.77	99.57	99.70
	SDV	N.A.	0.02	0.01	N.A.	N.A.
	TPL (W)	18.32	102.56	140.78	39.39	15.53
	SDV	N.A.	28.27	58.46	N.A.	N.A.
C	***TT (s)***	0.26	0.64	0.56	0.66	0.24

SDV	N.A.	0.14	0.11	N.A.	N.A.
TA (%)	98.75	96.75	96.68	95.39	99.60
SDV	N.A.	0.01	0.01	N.A.	N.A.
TPL (W)	13.72	52.03	91.65	27.82	12.17
SDV	N.A.	17.20	46.73	N.A.	N.A.

V. Conclusion

In this paper, an ANN-based GMPPT method is proposed. The proposed GMPPT method features high tracking speed and accuracy and does not require expensive irradiance sensors or temperature sensors. Also, it can be implemented with low-cost DSC since it does not require complicated calculations. To verify the effectiveness of the proposed method, the simulations of the 252 SPs, as well as the simulations and experiments of 3 complicated SPs are carried out respectively. According to the simulation results, the proposed method has the best performance among all methods in terms of ***TT***, ***TA***, and ***TPL*** for all the three tested SPs, which are: the ***TT*** 0.19 s, ***TA*** 99.99 %, and ***TPL*** 11.11 W, all are averaged values. For the simulated results of 252 SPs, the ***APE*** is 0.01 W, the $\boldsymbol{TT_{avg}}$ is 0.18 s, and the ***CT*** is 252, which indicates that the proposed method can correctly predict the GMPP positions of all 252 SPs. These values all rank first among the compared methods. Finally, the three PI of the proposed method are also the best among all the compared methods based on the experimental results, which are: the ***TT*** 0.21 s, ***TA*** 99.66 %, and ***TPL*** 12.58 W, all are averaged values.

References

[1] A. Ostadrahimi, Y. Mahmoud, "Novel Spline-MPPT Technique for Photovoltaic Systems Under Uniform Irradiance and Partial Shading Conditions," *IEEE Transactions on Sustainable Energy*, vol. 12, no. 1, pp. 524-532, Jan. 2021.

[2] C. Huang, L. Wang, Z. Zhang, R. S. C. Yeung, A. Bensoussan, H. S. H. Chung, "A Novel Spline Model Guided Maximum Power Point Tracking Method for Photovoltaic Systems," *IEEE Transactions on Sustainable Energy*, vol. 11, no. 3, pp. 1309-1322, Jul. 2020.

[3] X. Li, Y. Zhu, H. Wen, Y. Du, W. Xiao, "Reference-Voltage-Line-Aided Power Incremental Algorithm for Photovoltaic GMPPT and Partial Shading Detection," *IEEE Transactions on Sustainable Energy*, vol. 13, no. 3, pp. 1756-1770, Jul. 2022.

[4] M. P. Korukonda, R. Prakash, S. Samanta, L. Behera, "Model Free Adaptive Neural Controller for Standalone Photovoltaic Distributed Generation Systems With Disturbances," *IEEE Transactions on Sustainable Energy*, vol. 13, no. 2, pp. 653-667, Apr. 2022.

[5] A. M. Abomazid, N. A. E. Taweel, H. E. Z. Farag, "Optimal Energy Management of Hydrogen Energy Facility Using Integrated Battery Energy Storage and Solar Photovoltaic Systems," *IEEE Transactions on Sustainable Energy*, vol. 13, no. 3, pp. 1457-1468, Jul. 2022.

[6] M. Y. Javed, A. F. Murtaza, Q. Ling, S. Qamar, M. M. Gulzar, "A novel MPPT design using generalized pattern search for partial shading," *Energy and Buildings*, vol. 133, no. 1, pp. 59-69, Dec. 2016.

[7] R. Ramaprabha, M. Balaji, B. L. Mathur, "Maximum power point tracking of partially shaded solar PV system using modified Fibonacci search method with fuzzy controller," *International Journal of Electrical Power & Energy Systems*, vol. 43, no. 1, pp. 754-765, Dec. 2012.

[8] S. M. Hashemzadeh, "A new model-based technique for fast and accurate tracking of global maximum power point in photovoltaic arrays under partial shading conditions," *Renewable Energy*, vol. 139, no. 1, pp. 1061-1076, Aug. 2019.

[9] S. Xu, Y. Gao, G. Zhou, G. Mao, "A Global Maximum Power Point Tracking Algorithm for Photovoltaic Systems Under Partially Shaded Conditions Using Modified Maximum Power Trapezium Method," *IEEE Transactions on Industrial Electronics*, vol. 68, no. 1, pp. 370-380, Jan. 2021.

[10] T. L. Nguyen, K. S. Low, "A Global Maximum Power Point Tracking Scheme Employing DIRECT Search Algorithm for Photovoltaic Systems," *IEEE Transactions on Industrial Electronics*, vol. 57, no. 10, pp. 3456-3467, Oct. 2010.

[11] P. Bharadwaj, V. John, "Optimized Global Maximum Power Point Tracking of Photovoltaic Systems Based on Rectangular Power Comparison," *IEEE Access*, vol. 9, no. 1, pp. 53602-53616, Apr. 2021.

[12] K. Ishaque, Z. Salam, "A Deterministic Particle Swarm Optimization Maximum Power Point Tracker for Photovoltaic System Under Partial Shading Condition," *IEEE Transactions on Industrial Electronics*, vol. 60, no. 8, pp. 3195-3206, Aug. 2013.

[13] M. E. Başoğlu, B. Çakır, "A novel voltage-current characteristic based global maximum power point tracking algorithm in photovoltaic systems," *Energy*, vol. 112, no. 1, pp. 153-163, Oct. 2016.

[14] M. Boztepe, F. Guinjoan, G. V. Quesada, S. Silvestre, A. Chouder, E. Karatepe, "Global MPPT Scheme for Photovoltaic String Inverters Based on Restricted Voltage Window Search Algorithm," *IEEE Transactions on Industrial Electronics*, vol. 61, no. 7, pp. 3302-3312, Jul. 2014.

[15] A. A. Zadeh, M. Toulabi, A. S. Dobakhshari, S. T. Broujeni, A. M. Ranjibar, "A novel technique to extract the maximum power of photovoltaic array in partial shading conditions," *International Journal of Electrical Power & Energy Systems*, vol. 101, no. 1, pp. 500-512, Oct. 2018.

[16] A. W. Ibrahim, M. B. Shafik, M. Ding, M. A. Sarhan, Z. Fang, A. G. Alareqi, T. Almoqri, A. M. A. Rassas, "PV maximum power-point tracking using modified particle swarm optimization under partial shading conditions," *Chinese Journal of Electrical Engineering*, vol. 6, no. 4, pp. 106-121, Dec. 2020.

[17] S. Makhloufi, S. Mekhilef, "Logarithmic PSO-Based Global/Local Maximum Power Point Tracker for Partially Shaded Photovoltaic Systems," *IEEE Journal of Emerging and Selected Topics in Power Electronics*, vol. 10, no. 1, pp. 375-386, Apr. 2021.

[18] A. M. Eltamaly, "An Improved Cuckoo Search Algorithm for Maximum Power Point Tracking of Photovoltaic Systems under Partial Shading Conditions," *Energies*, vol. 14, no. 4, pp. 953, Feb. 2021.

[19] Y. P. Huang, M. Y. Huang, C. E. Ye, "A Fusion Firefly Algorithm With Simplified Propagation for Photovoltaic MPPT Under Partial Shading Conditions," *IEEE Transactions on Sustainable Energy*, vol. 11, no. 4, pp. 2641-2652, Oct. 2020.

[20] S. Motahhir, A. Chouder, A. E. Hammoumi, A. S. Benyoucef, A. E. Ghzizal, S. Kichou, K. Kara, P. Sanjeevikumar, S. Silvestre, "Optimal Energy Harvesting From a Multistrings PV Generator Based on Artificial Bee Colony Algorithm," *IEEE Systems Journal*, vol. 15, no. 3, pp. 4137-4144, Sep. 2021.

[21] K. Guo, L. Cui, M. Mao, L. Zhou, Q. Zhang, "An Improved Gray Wolf Optimizer MPPT Algorithm for PV System With BFBIC Converter Under Partial Shading," *IEEE Access*, vol. 8, no. 1, pp. 103476-103490, Jun. 2020.

[22] Y. H. Liu, J. H. Chen, J. W. Huang, "Global maximum power point tracking algorithm for PV systems operating under partially shaded conditions using the segmentation search method," *Solar Energy*, vol. 103, no. 1, pp. 350-363, May. 2014.

[23] S. A. Rizzo, G. Scelba, "ANN based MPPT method for rapidly variable shading conditions," *Applied Energy*, vol. 145, no. 1, pp. 124-132, May. 2015.

[24] M. Chen, S. Ma, "Analysis of MPPT Failure and Development of an Augmented Nonlinear Controller for MPPT of Photovoltaic Systems under Partial Shading Conditions," *Applied Sciences* vol. 7, no. 1, pp. 95, Jan. 2017.

[25] K. Punitha, D. Devaraj, S. Sakthivel, "Artificial neural network based modified incremental conductance algorithm for maximum power point tracking in photovoltaic system under partial shading conditions," *Energy*, vol. 62, no. 1, pp. 330-340, Dec. 2013.

[26] X. Meng, F. Gao, T. Xu, C. Zhang, "Fast Two-Stage Global Maximum Power Point Tracking for Grid-Tied String PV Inverter Using Characteristics Mapping Principle," *IEEE Journal of Emerging and Selected Topics in Power Electronics*, vol. 10, no. 1, pp. 564-574, Feb. 2022.

[27] S. Allahabadi, H. I. Eini, S. Farhangi, "Fast Artificial Neural Network Based Method for Estimation of the Global Maximum Power Point in Photovoltaic Systems," *IEEE Transactions on Industrial Electronics*, vol. 69, no. 6, pp. 5879-5888, Jul. 2022.

[28] H. M. E. Helw, A. Magdy, M. I. Marei, "A Hybrid Maximum Power Point Tracking Technique for Partially Shaded Photovoltaic Arrays" *IEEE Access*, vol. 5, no. 1, pp. 11900-11908, Jun. 2017.

[29] W. Zhang, G. Zhou, H. Ni, Y. Sun, "A Modified Hybrid Maximum Power Point Tracking Method for Photovoltaic Arrays Under Partially Shading Condition," *IEEE Access*, vol. 7, no. 1, pp. 160091-160100, Oct. 2019.
[30] Syafaruddin, E. Karatepe, T. Hiyama, "Artificial Neural Network-Polar Coordinated Fuzzy Controller Based Maximum Power Point Tracking Control Under Partially Shaded Conditions," *IET Renewable Power Generation*, vol. 3, no. 2, pp. 239-253, Jul. 2009.
[31] S. P. Ye, Y. H. Liu, S. C. Wang, H. Y. Pai, "A novel global maximum power point tracking algorithm based on Nelder-Mead simplex technique for complex partial shading conditions," *Applied Energy*, vol. 321, no. 1, pp. 119380, Sep. 2022.
[32] B. R. Peng, K. C. Ho, Y. H. Liu, "A Novel and Fast MPPT Method Suitable for Both Fast Changing and Partially Shaded Conditions," *IEEE Transactions on Industrial Electronics*, vol. 65, no. 4, pp. 3240-3251, Apr. 2018.